A Note on Dissipative Particle Dynamics (DPD) Modelling of Simple Fluids

N. Phan-Thien[1], N. Mai-Duy[2,*] and T.Y.N. Nguyen[2]
[1] Department of Mechanical Engineering, Faculty of Engineering,
National University of Singapore, 9 Engineering Drive 1, 117575, Singapore,
[2]Computational Engineering and Science Research Centre,
School of Mechanical and Electrical Engineering,
University of Southern Queensland, Toowoomba, QLD 4350, Australia.

ABSTRACT: In this paper, we show that a Dissipative Particle Dynamics (DPD) model of a viscous Newtonian fluid may actually produce a linear viscoelastic fluid. We demonstrate that a single set of DPD particles can be used to model a linear viscoelastic fluid with its physical parameters, namely the dynamical viscosity and the relaxation time in its memory kernel, determined from the DPD system at equilibrium. The emphasis of this study is placed on (i) the estimation of the linear viscoelastic effect from the standard parameter choice; and (ii) the investigation of the dependence of the DPD transport properties on the length and time scales, which are introduced from the physical phenomenon under examination. Transverse-current auto-correlation functions (TCAF) in Fourier space are employed to study the effects of the length scale, while analytic expressions of the shear stress in a simple small amplitude oscillatory shear flow are utilised to study the effects of the time scale. A direct mechanism for imposing the particle diffusion time and fluid viscosity in the hydrodynamic limit on the DPD system is also proposed.

Keywords: Dissipative particle dynamics (DPD); simple fluids; generalised hydrodynamics; Newtonian fluids; linear viscoelastic fluids

*Corresponding author E-mail: nam.mai-duy@usq.edu.au, Telephone +61-7-46312748, Fax +61-7-46312529

1   Introduction

In the dissipative particle dynamics (DPD) (e.g. [1]), the fluid is modelled by a system of particles undergoing their Newton 2nd law motions

$$m_i \ddot{\mathbf{r}}_i = m_i \dot{\mathbf{v}}_i = \sum_{j=1, j \neq i}^{N} \left(\mathbf{F}_{ij,C} + \mathbf{F}_{ij,D} + \mathbf{F}_{ij,R} \right), \tag{1}$$

where N is the number of particles, m_i, $\mathbf{r}_i$ and $\mathbf{v}_i$ the mass, position vector and velocity vector of a particle i, respectively, and $\mathbf{F}_{ij,C}$, $\mathbf{F}_{ij,D}$ and $\mathbf{F}_{ij,R}$ the conservative, dissipative and random forces, respectively,

$$\mathbf{F}_{ij,C} = a_{ij} w_C \mathbf{e}_{ij}, \tag{2}$$

$$\mathbf{F}_{ij,D} = -\gamma w_D \mathbf{e}_{ij} \cdot \mathbf{v}_{ij} \mathbf{e}_{ij}, \tag{3}$$

$$\mathbf{F}_{ij,R} = \sigma w_R \theta_{ij} \mathbf{e}_{ij}, \quad w_R = \sqrt{w_D}, \quad \sigma = \sqrt{2\gamma k_B T}, \tag{4}$$

in which a_{ij}, γ and σ are the amplitudes, and w_C, w_D and w_R, the weighting functions, with $\mathbf{e}_{ij} = \mathbf{r}_{ij}/r_{ij}$ the unit vector from particle j to particle i ($\mathbf{r}_{ij} = \mathbf{r}_i - \mathbf{r}_j$, $r_{ij} = |\mathbf{r}_{ij}|$), $\mathbf{v}_{ij} = \mathbf{v}_i - \mathbf{v}_j$ the relative velocity vector, $k_B T$ the Boltzmann temperature and θ_{ij} a Gaussian white noise. It is noted that the characteristics of the random force are defined by the fluctuation-dissipation theorem. In practice, one usually employs the weighting functions of the form

$$w_D = \left(1 - \frac{r}{r_c} \right)^s, \tag{5}$$

$$w_C = \left(1 - \frac{r}{r_c} \right), \tag{6}$$

where s is a positive value ($s = 2$ and $s = 1/2$: standard and modified values, respectively) and r_c the cut-off radius. The DPD input parameters include s, a_{ij}, σ, $k_B T$, m, r_c and the particle density n.

The DPD is thus a method of tracking particles in their motions, leading to the satisfaction of conservation equations (mass and momentum, or the Navier-Stokes [NS] equations) in the

mean - in that sense it is a bottom up approach to solving NS equations. It requires no prior specification of the constitutive relation for the fluid - the stress-strain rate relation is also obtained as a part of the solution procedure. It has been shown that, for preceding standard descriptions of the DPD interaction parameters, the DPD system is actually a Newtonian fluid on a long-time average [1]. In this work, we explore the generalised hydrodynamic regime of a DPD fluid that is defined by equations (1)-(6), where typical length scales include the interaction range r_c and the dynamic correlation length l_0 defined as $l_0 = v_0 t_0$ in which v_0 and t_0 are, respectively, the typical thermal velocity and collision time (or kinetic time) [1]

$$v_0 = \sqrt{\frac{k_B T}{m}}, \tag{7}$$

$$t_0 = \frac{1}{\omega_0}, \quad \omega_0 = \frac{n\,[w_D]\,\gamma}{3m}, \quad [w_D] = 4\pi r_c^3 \left[\frac{1}{1+s} - \frac{2}{2+s} + \frac{1}{3+s}\right]. \tag{8}$$

The classification of dynamic regimes in DPD can be based on the two length scales, r_c and l_0: "particle" regime when $r_c < l_0$ and "collective" regime when $r_c > l_0$. In this work, the focus is on a collective regime. Note that if one takes $n = \{3, 4\}$, $r_c = 1$, $m = 1$, $\sigma = 3$ and $k_B T = 1$ (commonly used input values), then the above estimates yield $l_0 = \{0.5305, 0.3979\}$ for $s = 2$ (standard DPD fluids) and $l_0 = \{0.1161, 0.087\}$ for $s = 1/2$ (modified DPD fluids), all less than $r_c = 1$.

Let λ be the wavelength ($k = 2\pi/\lambda$ is the wave number) of a perturbation in the hydrodynamics, which can be regarded as the length scale on which the physical phenomena under examination occur. On the other hand, the correlation length l_0 forms a scale on which the DPD transport coefficients are defined. As $k \to 0$ and the observation time scale is large, the system behaves like a continuum (the NS equations/hydrodynamics limit). At finite k, the system can be described by a linearised form of the NS equations, where local deviations of the macroscopic variables (the number density and momentum density) from their average values are assumed to be small. As discussed in [2], a standard hydrodynamic regime occurs on the range $l_0 < r_c < \lambda$ while a mesoscopic hydrodynamic regime on $l_0 < \lambda < r_c$. In addition, there is a smooth transition between these two hydrodynamic regimes, which occurs at about $k_c = 2\pi/r_c$. The generalised hydrodynamics cover both the standard and the

mesoscopic hydrodynamics and thus can be probed by considering linearised NS equations induced by perturbations. The transport coefficients are now functions of k, and their values at $k = 0$ can be estimated through extrapolation. The regime of generalised hydrodynamics is particularly relevant in the simulation of complex fluids such as colloidal suspensions. In practice, an effective way to predict the DPD transport coefficients over a wide range of k is to employ the transverse-current autocorrelation functions (TCAF) in Fourier space [1,2].

Let ω be a characteristic frequency ($T = 1/\omega$ is a characteristic time). Assume that our (non-Newtonian) fluid in question has a characteristic time scale λ_t. If $T \gg \lambda_t$, the observation time scale is large and the material responds like a fluid; otherwise, one may have a solid-like response. For a linear viscoelastic fluid, the stress at the current time is dependent not only on the current strain rate but also the past strain rate; in 1D,

$$\sigma(t) = \int_{\gamma(-\infty)}^{\gamma(t)} G(t - t')d\gamma(t') = \int_{-\infty}^{t} G(t - t')\dot{\gamma}dt', \tag{9}$$

where $\dot{\gamma}$ is the shear rate (γ is the shear strain) and G is a decreasing function of time, the relaxation modulus. In the case of a simple shear flow, the stress analysis can be done in an exact manner. One can utilise its analytic solution to examine the effects of the frequency on the DPD transport properties.

One particular concern here is how to make a direct link between the fluid physical parameters and the (input) DPD parameters. We attempt to derive, by means of kinetic theory [1] and by using generalised forms of the dissipative weighting function, the relation between the particle diffusion time and the viscosity of the fluid (at the hydrodynamic limit), and the DPD parameters. The resultant analytic expressions allow one to specify these two physical parameters as the input parameters.

The remainder of the paper is organised as follows. In Sections 2 and 3, brief reviews of TCAF and analytic expressions of the shear stress in a simple small amplitude oscillatory shear flow are respectively given. In Section 4, we investigate the dependence of the DPD transport properties on the length scale and time scale on which the physical phenomena occur. In Section 5, we discuss how to impose the particle diffusion time and the viscosity in

4

the hydrodynamic limit on the DPD system, and quantify the linear viscoelastic effect from the standard parameter choice. Numerical experiments are presented in Section 6. Section 7 provides some concluding remarks.

2   Time current autocorrelation functions

The current density is given by

$$\mathbf{j}(\mathbf{r}, t) = \sum_{j=1}^{N} \mathbf{v}_j \delta(\mathbf{r} - \mathbf{r}_j(t)), \tag{10}$$

where N is the number of particles and subscripts j denote particle number. Since there is no overall motion, $\langle \mathbf{j}(\mathbf{r}, t) \rangle = 0$ ($< \cdot >$ denoted the average operation). Note that $\mathbf{j}(\mathbf{r}, t)$ is the macroscopic (hydrodynamic) variable and $\mathbf{v}$ the microscopic variable. The Fourier transformation of (10) is

$$\mathbf{J}(\mathbf{k}, t) = \int d\mathbf{r} \exp(i\mathbf{k} \cdot \mathbf{r}) \mathbf{j}(\mathbf{r}, t) = \sum_{j} \mathbf{v}_j(t) \exp(i\mathbf{k} \cdot \mathbf{r}_j(t)). \tag{11}$$

The spatial correlation function is defined as [3,4]

$$C_{\alpha\beta}(\mathbf{k}, t) = \frac{k^2}{N} \langle J_\alpha(-\mathbf{k}, 0) J_\beta(\mathbf{k}, t) \rangle, \tag{12}$$

where α and β denote Cartesian indices.

For an isotropic fluid, the correlation function (12) depends only on the magnitude of $\mathbf{k}$ and one can decompose it into the longitudinal ($\parallel$) and transverse ($\perp$) components relative to $\mathbf{k}$ as

$$C_{\alpha\beta}(k, t) = \frac{k_\alpha k_\beta}{k^2} C_{\parallel}(k, t) + \left(\delta_{\alpha\beta} - \frac{k_\alpha k_\beta}{k^2} \right) C_{\perp}(k, t), \tag{13}$$

where $\delta_{\alpha\beta}$ is the Kronecker delta, and

$$C_\perp(k,t) = \frac{k^2}{N}\langle J_\perp(-\mathbf{k},0)J_\perp(\mathbf{k},t)\rangle, \tag{14}$$

$$C_\parallel(k,t) = \frac{k^2}{N}\langle J_\parallel(-\mathbf{k},0)J_\parallel(\mathbf{k},t)\rangle. \tag{15}$$

3 Analytic solutions for simple shear flows of linear viscoelastic fluids

Here we recall some terminologies by considering a small amplitude oscillatory shear flow of a viscoelastic fluid. The flow is generated between two parallel plates separated by a distance h. The bottom plate is fixed while the top plate is sinusoidally displaced by $\delta\sin(\omega t)$ with $\delta \ll h$ being the small amplitude displacement in the x direction. The top plate velocity is

$$U(t) = \delta\omega\cos\omega t. \tag{16}$$

The shear rate and the shear strain experienced by the fluid are, respectively,

$$\dot\gamma(t) = \frac{\delta}{h}\omega\cos\omega t = \dot\gamma_0\cos\omega t, \tag{17}$$

$$\gamma(t) = \frac{\delta}{h}\sin\omega t = \gamma_0\sin\omega t, \quad \gamma_0 = \frac{\delta}{h} \ll 1, \quad \dot\gamma_0 = \omega\gamma_0. \tag{18}$$

For a linear viscoelastic fluid at any arbitrary amplitude δ, or for any viscoelastic fluid at a small enough amplitude δ, the only non-zero component of the stress is the shear stress

$$
\begin{aligned}
\tau_{xy} &= \int_{-\infty}^t G(t-t')\frac{\partial u_x(y,t')}{\partial y}dt' = \int_{-\infty}^t G(t-t')\dot\gamma_0\cos\omega t'dt', \\
&= \int_0^\infty \dot\gamma_0 G(s)\cos\omega(t-s)ds, \\
&= \int_0^\infty \dot\gamma_0 G(s)[\cos\omega t\cos\omega s + \sin\omega t\sin\omega s]ds, \\
&= G'(\omega)\gamma_0\sin\omega t + \eta'(\omega)\dot\gamma_0\cos\omega t, \\
&= G'(\omega)\gamma + \eta'(\omega)\dot\gamma = \text{elastic part} + \text{viscous part},
\end{aligned}
\tag{19}
$$

where $G'(\omega)$ is the storage modulus and $\eta'(\omega)$ is dynamic viscosity; they are related to the relaxation modulus $G(t)$ by

$$G'(\omega) = \int_0^\infty \omega G(s) \sin(\omega s) ds, \tag{20}$$

$$\eta'(\omega) = \int_0^\infty G(s) \cos(\omega s) ds. \tag{21}$$

By rewriting (19) as

$$\tau_{xy} = G'(\omega)\gamma_0 \sin\omega t + \eta'(\omega)\dot{\gamma}_0 \sin(\frac{\pi}{2} + \omega t), \tag{22}$$

the shear stress is shown to have the same phase as the applied strain for the elastic part, but $\pi/2$) out of phase from the applied strain for the viscous part. All of the foregoing are familiar results in continuum mechanics (e.g. [5]).

4 Generalised DPD transport coefficients

The conservation laws for the mass density $\rho(\mathbf{r}, t)$ and momentum density $m\mathbf{u}(\mathbf{r}, t)$ in the continuum description read

$$\frac{\partial\rho(\mathbf{r}, t)}{\partial t} + \nabla \cdot (\rho(\mathbf{r}, t)\mathbf{u}(\mathbf{r}, t)) = 0, \tag{23}$$

$$\frac{\partial}{\partial t}\rho(\mathbf{r}, t)\mathbf{u}(\mathbf{r}, t) + \mathbf{u}(\mathbf{r}, t) \cdot \nabla (\rho(\mathbf{r}, t)\mathbf{u}(\mathbf{r}, t)) + \nabla \cdot \boldsymbol{\sigma}(\mathbf{r}, t) = \mathbf{0}, \tag{24}$$

where $\boldsymbol{\sigma}$ is a stress tensor.

4.1 Newtonian fluids

In this case, the stress tensor is given by

$$\sigma_{\alpha\beta}(\mathbf{r}, t) = \delta_{\alpha\beta}p(\mathbf{r}, t) - \eta \left(\frac{\partial u_\alpha(\mathbf{r}, t)}{\partial r_\beta} + \frac{\partial u_\beta(\mathbf{r}, t)}{\partial r_\alpha} \right) - \delta_{\alpha\beta}\nabla \cdot \mathbf{u}(\mathbf{r}, t) \left(\eta_B - \frac{2}{3}\eta \right), \tag{25}$$

where p is the local pressure, η the shear viscosity and η_B the bulk viscosity.

Without applied external forces, one has $\langle \mathbf{u}(\mathbf{r},t) \rangle = 0$. Assume that local deviations of the hydrodynamic variables from their average values are small, the variables in (23), (24) and (25) can be expressed as [3,4]

$$n(\mathbf{r},t) = n + \delta n(\mathbf{r},t) \approx n, \tag{26}$$

$$\mathbf{u}(\mathbf{r},t) = \langle \mathbf{u}(\mathbf{r},t) \rangle + \delta \mathbf{u}(\mathbf{r},t) = \delta \mathbf{u}(\mathbf{r},t), \tag{27}$$

$$\rho \mathbf{u}(\mathbf{r},t) = m(n + \delta n(\mathbf{r},t))(\langle \mathbf{u}(\mathbf{r},t) \rangle + \delta \mathbf{u}(\mathbf{r},t)) \approx mn\delta \mathbf{u}(\mathbf{r},t) = mn\mathbf{u}(\mathbf{r},t) = \rho \mathbf{j}(\mathbf{r},t), \tag{28}$$

where high-order terms have been ignored and n is the equilibrium number density of the system. At equilibrium, the variables $< \delta n(\mathbf{r},t) >$ and $< \delta \mathbf{u}(\mathbf{r},t) >$ disappear.

Making use of (25) and (26)-(28), the conservation equations (23) and (24) reduce to the following linear form of the Navier-Stokes equation

$$\frac{\partial \delta \rho(\mathbf{r},t)}{\partial t} + \nabla \cdot \rho \mathbf{j}(\mathbf{r},t) = 0, \tag{29}$$

$$\frac{\partial \mathbf{j}(\mathbf{r},t)}{\partial t} + \frac{1}{\rho}\nabla p(\mathbf{r},t) - \frac{\eta}{\rho}\nabla^2 \mathbf{j}(\mathbf{r},t) - \frac{1}{\rho}\left(\eta_B + \frac{1}{3}\eta\right)\nabla\nabla \cdot \mathbf{j}(\mathbf{r},t) = \mathbf{0}. \tag{30}$$

In Fourier space, they become

$$\frac{\partial \delta \rho(\mathbf{k},t)}{\partial t} + i\mathbf{k} \cdot \rho \mathbf{J}(\mathbf{k},t) = 0, \tag{31}$$

$$\frac{\partial \mathbf{J}(\mathbf{k},t)}{\partial t} + ic^2 \rho(\mathbf{k},t)\mathbf{k} + \frac{\eta_k k^2}{\rho}\mathbf{J}(\mathbf{k},t) + \frac{1}{\rho}\left(\frac{4\eta_k}{3} + \eta_B\right)\mathbf{k}\mathbf{k} \cdot \mathbf{J}(\mathbf{k},t) = \mathbf{0}, \tag{32}$$

where c is the isothermal sound speed, and the viscosity becomes a function of the wave number, denoted by η_k.

For the shear viscosity, one only needs to consider the transverse component of the current density. Equation (32) reduces to

$$\frac{\partial J_\perp(\mathbf{k},t)}{\partial t} + \frac{\eta_k k^2}{\rho}J_\perp(\mathbf{k},t) = 0. \tag{33}$$

8

Note that equations (29)-(32) and (33) are valid for slow variations of the hydrodynamic dynamic variables only.

Multiplying both sides of (33) with $J_\perp(-\mathbf{k}, t)$ and then averaging,

$$\frac{\partial}{\partial t}C_\perp(k,t) + \frac{\eta_k k^2}{\rho}C_\perp(k,t) = 0, \tag{34}$$

whose solution is

$$\frac{C_\perp(k,t)}{C_\perp(k,0)} = \exp\left[-\frac{\eta_k k^2 t}{\rho}\right], \tag{35}$$

from which the viscosity in the Fourier-transformed space can be estimated from equilibrium correlation function data. With this approximation, the observation time scale is assumed to be large. The stress approximations, which involve an additional characteristic time scale, are discussed in next section.

4.2   Linear viscoelastic fluids

The stress tensor for a linear viscoelastic fluid takes the form

$$\sigma_{\alpha\beta}(\mathbf{r},t) = \int_{-\infty}^{t} dt' G(t-t')\left(\frac{\partial u_\alpha(\mathbf{r},t')}{\partial r_\beta} + \frac{\partial u_\beta(\mathbf{r},t')}{\partial r_\alpha}\right), \tag{36}$$

where $G(t)$ is the relaxation modulus, a decreasing function of time. The stress at the current time is thus dependent on both the current and past strain rates. It can be seen that, (i) the contribution of a strain rate at the distant past is weighted by the memory relaxation modulus and is less than that of a more recent strain rate (i.e. the concept of fading memory); and (ii) when the memory function is chosen as a Dirac delta function (i.e. $G(t-t') = \eta\delta(t-t')$), a Newtonian fluid is recovered.

Here, we consider a simple relaxation modulus (the Maxwell relaxation modulus)

$$G(t-t') = \frac{\eta}{\tau}\exp\left(-\frac{t-t'}{\tau}\right), \tag{37}$$

where τ is a Maxwell relaxation time/decay constant. A fit to the equilibrium normalised

$C_\perp(k, t)$ data is now described as a function of not only the viscosity η but also the decay constant of the memory function, τ. From continuum mechanics, a plane wave given by $\mathbf{u} = (u_0 \cos ky, 0, 0)$ will decay according to

$$\frac{\partial u_x(y, t)}{\partial t} = \frac{\eta}{\tau \rho} \int_0^t dt' \exp\left(-\frac{t - t'}{\tau}\right) \frac{\partial^2 u_x(y, t')}{\partial y^2}, \tag{38}$$

which can be derived from the NS equations. An exact solution to (38) is

$$u_x(y, t) = u_0 \exp\left(-\frac{t}{2\tau}\right) \left(\cosh \frac{\Omega t}{2\tau} + \frac{1}{\Omega} \sinh \frac{\Omega t}{2\tau}\right) \cos ky, \tag{39}$$

where

$$\Omega = \sqrt{1 - 4\frac{\tau \eta k^2}{\rho}}. \tag{40}$$

On the other hand, from a DPD point of view and without an initial plane wave applied, thermal fluctuations still occur in a system at a given temperature. Since the response of the system to internal fluctuations is the same as to external perturbations, one can link the TCAF to (39), resulting in [6]

$$\frac{C_\perp(k, t)}{C_\perp(k, 0)} = \exp\left(-\frac{t}{2\tau_k}\right) \left(\cosh \frac{\Omega_k t}{2\tau_k} + \frac{1}{\Omega_k} \sinh \frac{\Omega_k t}{2\tau_k}\right), \tag{41}$$

where $\tau_k = \tau(k)$ and Ω_k is defined as in (40) with $\tau = \tau_k$ and $\eta = \eta_k$. This model involves two fitting parameters, namely the decay time τ_k and the dynamical viscosity η_k. Alternatively, as discussed in [7], the two fitting parameters can be chosen as the decay times of the memory function (τ_k) and TCAF (τ_k^*), and the fitting model is also shown to be in the form of (41) with Ω_k being defined as $\Omega_k^2 = (1/2\tau_k)^2 - (1/\tau_k \tau_k^*)^2$ and the relation between the viscosity and the decay time of TCAF as $\eta_k = \rho/k^2 \tau_k^*$.

For each value of k, we fit the model (41) to the equilibrium correlation function data. To examine the dependence of the DPD transport properties on the frequency ω, we now utilise analytical expressions of the shear stress in a simple oscillatory flow with a small applied strain. Using (20) and (21), the coefficients in the strain, $G'(\omega)$, the storage modulus, and

in the strain rate, $\eta'(\omega)$, the dynamic viscosity are computed as

$$G'(\omega) = \int_0^\infty \omega G(s) \sin(\omega s) ds = \int_0^\infty \omega \frac{\eta_k}{\tau_k} \exp\left(-\frac{s}{\tau_k}\right) \sin(\omega s) ds = \frac{\eta_k \omega^2 \tau_k}{\omega^2 \tau_k^2 + 1}, \tag{42}$$

$$\eta'(\omega) = \int_0^\infty G(s) \cos(\omega s) ds = \int_0^\infty \frac{\eta_k}{\tau_k} \exp\left(-\frac{s}{\tau_k}\right) \cos(\omega s) ds = \frac{\eta_k}{\tau_k^2 \omega^2 + 1}, \tag{43}$$

where $s = t - t'$. With the storage modulus and shear viscosity being functions of the frequency, one now has an effective mechanism for investigating the response of the DPD system: purely viscous ($\omega \to 0$), purely elastic ($\omega \to \infty$) and viscoelastic (intermediate values of ω).

It can be seen from (42) and (43) that

$$G'(\omega) \to 0 \text{ and } \eta'(\omega) \to \eta_k \text{ as } \omega \to 0, \tag{44}$$

$$G'(\omega) \to \frac{\eta_k}{\tau_k} \text{ and } \eta'(\omega) \to 0 \text{ as } \omega \to \infty. \tag{45}$$

5   Imposition of fluid properties

One main drawback of the classical DPD formulation is that there is no direct link between the DPD input parameters and the macroscopic properties of the fluid. Here, we show that it is possible to directly impose the particle diffusion time and the viscosity of the fluid in the hydrodynamic limit on the DPD system with the dissipative weighting function of a generalised form, i.e. $w_D = (1 - r/r_c)^s$.

The viscosity of the fluid, η, can be specified as an input parameter by enforcing the following constraint [8,9]

$$\eta = \frac{\gamma n^2 [R^2 w_D]_R}{30} = \frac{\gamma n^2}{30} \frac{96 \pi r_c^5}{(s+1)(s+2)(s+3)(s+4)(s+5)}, \tag{46}$$

where right hand is the dissipative part of the total viscosity by the kinetic theory [1]. This

equation can be solved for the DPD parameter γ,

$$\gamma = \frac{5\eta(s+1)(s+2)(s+3)(s+4)(s+5)}{16\pi n^2 r_c^5},$$ (47)

which is equation (44) in [9].

The particle diffusion time can be defined as the time taken by the particle to diffuse a distance equal to its radius (the time to restore the equilibrium configuration)

$$\tau_P = \frac{R^2}{D},$$ (48)

where R is the radius and D the self-diffusion coefficient of a particle.

Consider a tagged particle in a sea of other particles. Its radius can be estimated by the Stokes-Einstein relation

$$R = \frac{k_B T}{6\pi D \eta}.$$ (49)

Substitution of (49) into (48) yields

$$\tau_P = \frac{(k_B T)^2}{36\pi^2 D^3 \eta^2}.$$ (50)

By means of kinetic theory, an analytic expression for the diffusivity can be derived as

$$D = \frac{3mk_B T}{\gamma mn[w_D]_R} = \frac{3mk_B T}{\gamma mn}\frac{(s+1)(s+2)(s+3)}{8\pi r_c^3},$$ (51)

(i.e. equation (36) in [9]) and expression (50) becomes

$$\tau_P = \frac{(k_B T)^2}{36\pi^2 \eta^2}\left(\frac{8\pi r_c^3 \gamma n}{3k_B T(s+1)(s+2)(s+3)}\right)^3.$$ (52)

Substitution of (47) into (52) yields the following quadratic equation

$$s^2 + 9s + 20 - E = 0, \quad E = \frac{6k_B T n r_c^2}{5\eta}\sqrt[3]{\frac{36\pi^2 \eta^2 \tau_P}{k_B T^2}},$$ (53)

which always has two real solutions and we are interested in the positive one

$$s = \frac{-9 + \sqrt{1 + 4E}}{2}, \quad E > 20. \tag{54}$$

The requirement $E > 20$ leads to

$$\tau_P > \frac{31250}{243\pi^2} \frac{\eta}{k_B T n^3 r_c^6} \text{ for a given } \eta, \tag{55}$$

$$\eta < \frac{243\pi^2}{31250} k_B T n^3 r_c^6 \tau_P \text{ for a given } \tau_P. \tag{56}$$

For given values of τ_P and η, satisfying the conditions (55) and (56), values of s and γ can then be computed from (54) and (47), respectively. According to the kinetic theory, the two physical parameters τ_P and η will take the specified values for the values of r_c, $k_B T$, n and m employed.

The DPD without energy conservation describes an isothermal fluid that can be characterised through the mass density $\rho = mn$, viscosity η and Schmidt number $S_c = \eta/\rho D$. It is convenient to rewrite the particle diffusion time (50) in the form

$$\tau_P = \frac{1}{36\pi^2} \frac{\rho^3 S_c^3 (k_B T)^2}{\eta^5}. \tag{57}$$

In investigating the effects of τ_P, we keep values of ρ, η and S_c constant. In DPD, $k_B T$ is simply a specific kinetic energy; by changing $k_B T$, one can vary the input τ_P. Here, we are interested the relation between the particle diffusion time and the relaxation time of the memory kernel (37) - it will be studied numerically in next section.

6 Numerical results

From the DPD equilibrium state space (time-varying positions and velocities of particles), the viscosity can be extracted for different wave numbers. For each wave number, several sets of values of $C_\perp(k,t)/C_\perp(k,0)$ can be calculated from the DPD simulation data; these can be employed for fitting and back tracking the physical parameters. We use the fitting

model (35) and (41) for Newtonian and viscoelastic fluids, respectively.

Consider a DPD system defined on a domain of $15 \times 15 \times 15$ with periodic boundary conditions, and ($a_{ij} = 3.5328$, $n = 4$, $r_c = 1.5$, $k_B T = 1$, $m = 1$, $\Delta t = 0.001$). Its physical input parameters (fluid properties) chosen to be imposed are $\eta = 30$ and $Sc = 500$, which correspond to the original input parameters: $\gamma = 6.9710$ and $s = 0.4244$ [9]. It can be seen that the value of s used here is close to 0.5 (the modified DPD fluid), and the corresponding dynamical correlation length ($l_0 = 0.0149$) is less than $r_c = 1.5$. We apply the modified velocity-Verlet algorithm [10] to solve the DPD equations of motion. Here, the wave number is chosen in the range of 0.4189 to 7.1209 (i.e. 17 values) and their associated results are obtained from a single run. A run of 5×10^5, 1.5×10^6, 2×10^6 time steps produces, respectively, 15, 46 and 62 data sets. For each data set, TCAFs are obtained by averaging 500 overlapping samples in which measurements are made every 5 time steps and there are 1025 measurements per sample. It is observed that using a larger number of data sets make the solution behaviour with respect to the wave number more stable. In the following sections, the obtained results from 62 data sets are presented. Both Newtonian and viscoelastic fitting models are applied to the same TCAF data (i.e. $C_\perp(k,t)/C_\perp(k,0)$). Their resultant curve fits are observed to be graphically the same; only those for the Newtonian case are displayed. For a time step, the elapsed CPU time of computing TCAF is insignificant compared to that of solving the DPD equations of motion.

6.1   Newtonian fluids

Some typical variations of TCAF are displayed in Figures 1. Since the finite size, defined through wavelength, is taken into account, the Newtonian viscosity estimated from TCAF is a function of the wave number. The obtained results are shown in Figures 2 and 3. One has a wave number-dependent viscosity with the observation time scale being assumed to be large. To obtain the viscosity at $k = 0$ (a continuum), some extrapolation is needed. As discussed in [11], η_k must be an even function of k and thus may be approximated as

$$\eta_k = \eta_0 + ak^2, \tag{58}$$

14

where η_0 and a are two fitting parameters. Assuming that values of k used for the fitting are sufficiently small, η_0 can be regarded as the viscosity at the hydrodynamic limit. Using the first 4 smallest values of k (i.e. 0.4189, 0.8378, 1.2566 and 1.6755), this leads to $\eta_0 = 29.0214$. On the other hand, from the kinetic theory [1], the viscosity is estimated as $\eta = 30$. The advantage of the TCAF approach is that it can provide information about the size effect on the transport properties. In addition, one can estimate the transport coefficients at the hydrodynamic limit through extrapolation.

6.2 Linear viscoelastic fluids

6.2.1 Wavelength- and frequency-dependent transport coefficients

The stress approximations involve two parameters, the viscosity and relaxation time, which are wavelength- and frequency-dependent.

Figure 4 shows plots of the viscosity and the decay constant of the memory function against the wave number k. When k decreases, the decay constant τ_k is seen to increase quickly and is expected to reach its maximum in the hydrodynamic limit. For the shear viscosity η_k, the change is observed to be slow as $k \to 0$. The obtained values of η_k here are similar to those in the Newtonian case.

Figure 5 displays the storage modulus and viscosity against the frequency ω, according to (42) and (43), for the first (smallest) value of k (i.e. $k = k_1 = 0.4189$). At small values of the frequency (i.e. large observation time scale), the system responses like a fluid and at large values of the frequency, one has a solid-like response. The storage modulus provides a convenient means of quantifying the level of elasticity of the fluid.

Figure 6 displays the shear viscosity against the frequency ω for the first four values of k (i.e. 0.4189, 0.8378, 1.2566 and 1.6755). It can be seen that $\eta' \to \eta_k$ as $\omega \to 0$ and $\eta' \to 0$ as $\omega \to \infty$.

Figure 7 displays the storage modulus against the frequency ω for the first four values of k.

It can be seen that $G' \to 0$ as $\omega \to 0$ and $G' \to \eta_k/\tau_k$ as $\omega \to \infty$.

6.2.2 Linear viscoelastic effect

As shown above, a DPD model using a single set of particles can result in a linear viscoelastic fluid for $k \geq 0$. A concern here is how to quantify the linear viscoelastic effect. Some typical scenarios are studied below and some comments are given at the end of this section. Table 1 displays values of the original DPD parameters γ and s that correspond to the input viscosities and Schmidt numbers imposed here.

Same fluid at different imposed $k_B T$

Five values of $k_B T$, (1, 1.1, 1.2, 1.3, 1.4), are employed in conjunction with ($\rho = 4$, $S_c = 500$ and $\eta = 30$). They lead to $\tau_P = (0.93, 1.12, 1.33, 1.57, 1.82)$, respectively, according to (57). The obtained results concerning the effects of the particle diffusion time τ_P on the relaxation time of the memory kernel, τ_k, over a wide range of k are shown in Figure 8.

Fluids of different viscosities

Four values of η, (30, 28, 26, 24), are employed in conjunction with ($\rho = 4$, $S_c = 500$ and $k_B T = 1$). Figure 9 shows the effects of the imposed viscosity η on the relaxation time τ_k over a wide range of k.

Fluids of different Schmidt numbers

Four values of S_c, (500, 600, 700, 800), are employed in conjunction with ($\rho = 4$, $\eta = 30$ and $k_B T = 1$). Figure 10 shows the effects of the imposed limit Schmidt number S_c on the relaxation time τ_k over a wide range of k.

From the three figures, it can be seen that the relaxation time, corresponding to different values of τ_P, η or S_c, apparently converges as k is reduced, and one would expect that an extrapolation will lead to a similar value for the relaxation time in the limit $k \to 0$. At finite k, the obtained results suggest that the relaxation time can be strongly affected by

16

the particle diffusion time, viscosity or Schmidt number. An increase in τ_P, a decrease in η or an increase in S_c results in a decrease in τ_k. Differences of τ_k at small k are thus much smaller than those at large k. It can also been seen that a change in S_c or τ_P can affect the estimated viscosity at the hydrodynamic limit.

7 Concluding remarks

In this work, DPD in its generalised hydrodynamic regime is considered. For a Newtonian fluid, the stresses are obtained through a large-time averaging process; they involve one fitting parameter, namely the viscosity, which is wavelength-dependent. For a linear viscoelastic fluids, the stresses involve two fitting parameters, namely the viscosity and the relaxation time, which are wavelength- and frequency-dependent. The wavelength dependency of the transport coefficients is obtained numerically while their frequency dependency can be computed analytically, which allow the effects of the length and time scales introduced by physical phenomena to be determined. The DPD input parameters can be determined from the viscosity, mass density, Schmidt number and diffusion time. Numerical experiments indicate that (i) a fluid modelled from a single set of particles may not be Newtonian, but linear viscoelastic, and any time dependent effects must be carefully looked at, and (ii) the relaxation time measuring the linear viscoelastic effect can be adjusted by means of the input diffusion time, viscosity or Schmidt number at finite wave numbers.

References

1. Marsh C. Theoretical Aspects of Dissipative Particle Dynamics (D. Phil. Thesis). University of Oxford; 1998.

2. Ripoll M, Ernst MH, Español P. Large scale and mesoscopic hydrodynamics for dissipative particle dynamics. J Chem Phys 2001;115(15):7271-7284.

3. Boon JP, Yip S. Molecular Hydrodynamics. New York: Dover Publications Inc; 1991.

4. Hansen JP, McDonald IR. Theory of Simple Liquids. 3rd ed. London: Academic Press; 2006.

5. Phan-Thien N, Mai-Duy N. Understanding Viscoelasticity: An Introduction to Rheology. 3rd ed. Cham (Switzerland): Springer International Publishing; 2017.

6. Hess B. Determining the shear viscosity of model liquids from molecular dynamics simulations. J Chem Phys 2002;116(1):209-217.

7. Vogelsang R, Hoheisel C. Computation and analysis of the transverse current autocorrelation function, C_t(k,t), for small wave vectors: A molecular-dynamics study for a Lennard-Jones fluid. Phys Rev A 1987;35(4):1786-1794.

8. Mai-Duy N, Phan-Thien N, Tran-Cong T. An improved dissipative particle dynamics scheme. Appl Math Model 2017;46:602-617.

9. Mai-Duy N, Phan-Thien N, Tran-Cong T. Imposition of physical parameters in dissipative particle dynamics. Comput Phys Comm 2017;221:290-298.

10. Groot RD, Warren PB, Dissipative particle dynamics: Bridging the gap between atomistic and mesoscopic simulation, J Chem Phys 1997;107:4423-4435.

11. Palmer BJ. Transverse-current autocorrelation-function calculations of the shear viscosity for molecular liquids. Phys Rev E 1994;49(1):359-366.

Table 1: Values of the input viscosity and Schmidt number, and the corresponding original DPD parameters for $(m = 1, n = 4, k_BT = 1, r_c = 1.5)$.

Physical inputs		Original DPD parameters	
η	S_c	γ	s
30	500	6.9710	0.4244
28	500	11.7110	0.7727
26	500	19.6042	1.1747
24	500	32.9714	1.6441
30	600	15.0263	0.8898
30	700	27.4087	1.3181
30	800	44.9254	1.7169
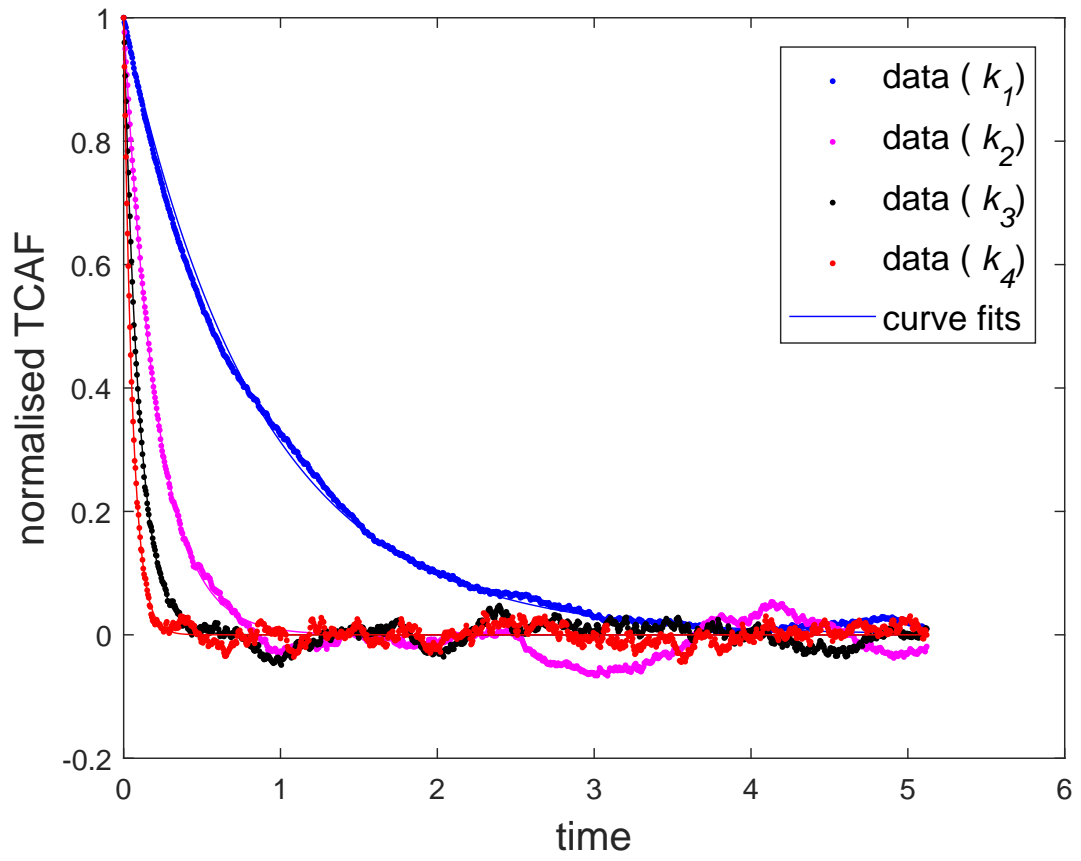
Figure 1: Newtonian fluids: Calculated values of TCAF and their curve fits (solid lines) by using (35) for the four smallest k values.
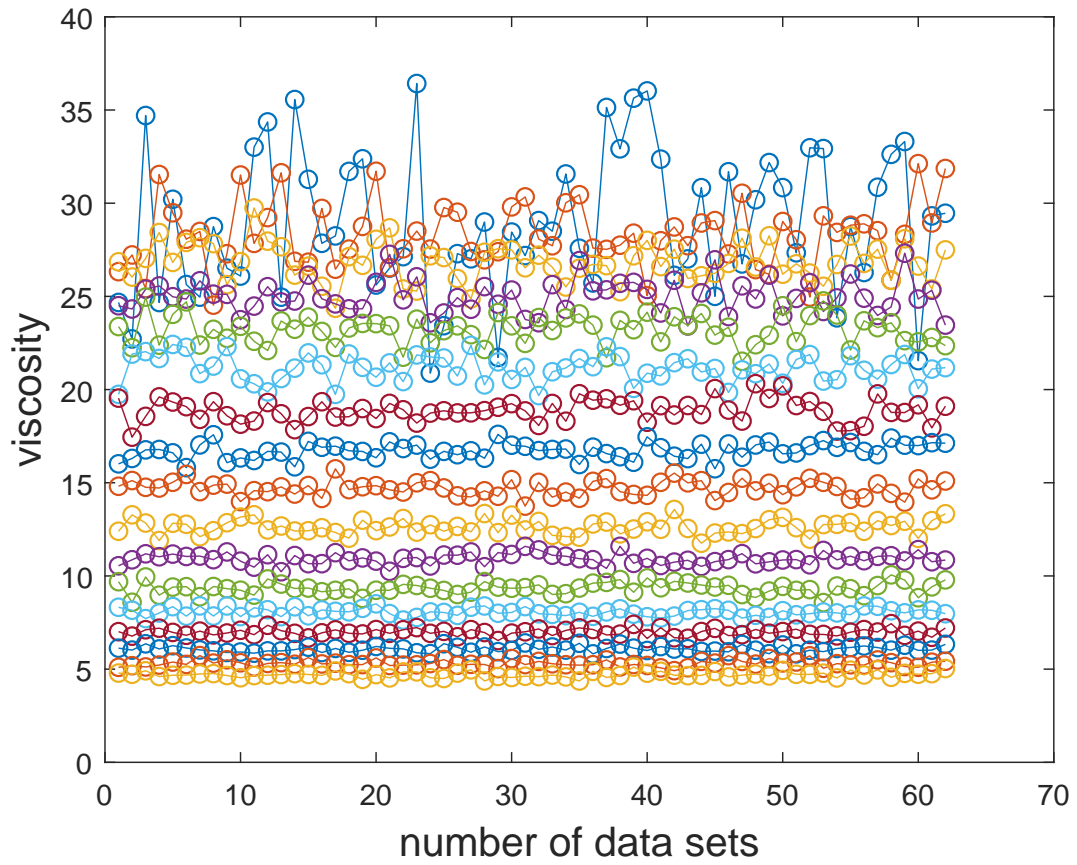
Figure 2: Newtonian fluids: Several data sets are used for obtaining the viscosity. Its deviation is generally reduced with increasing k value (i.e. top to bottom).
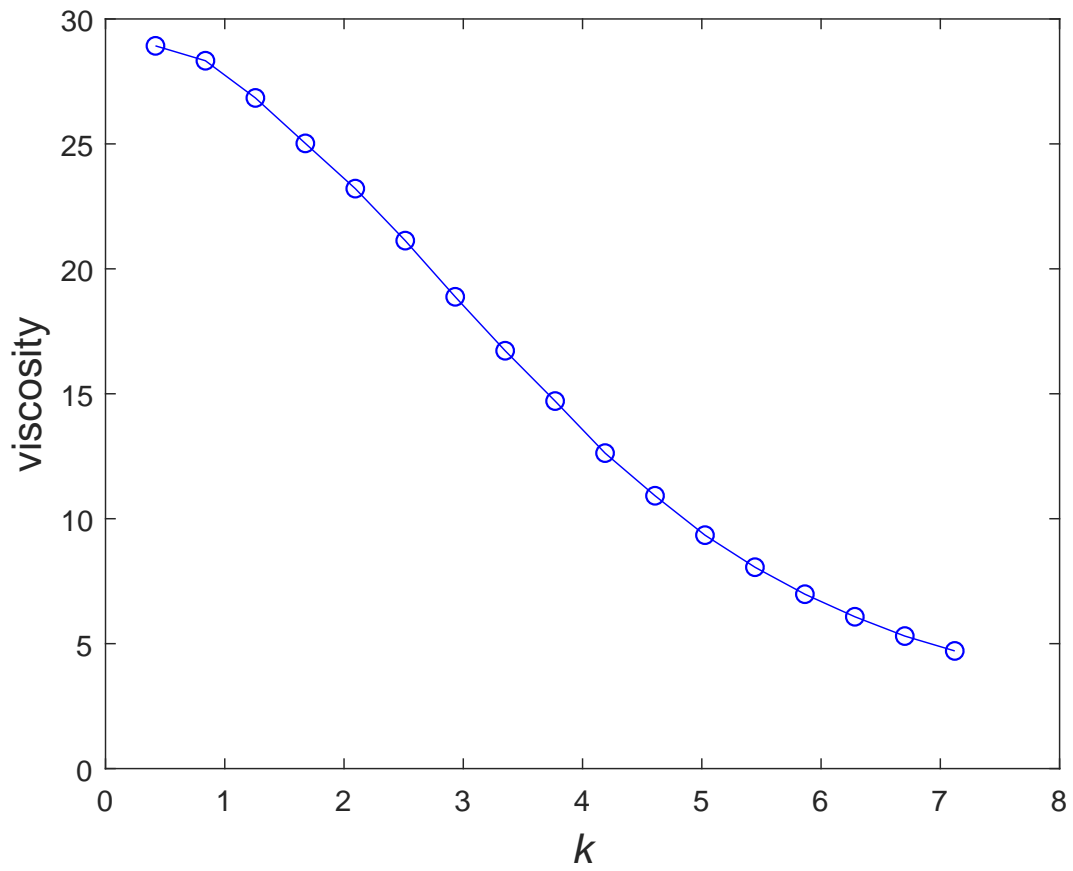
Figure 3: Newtonian fluids: Viscosity as a function of the wave number.
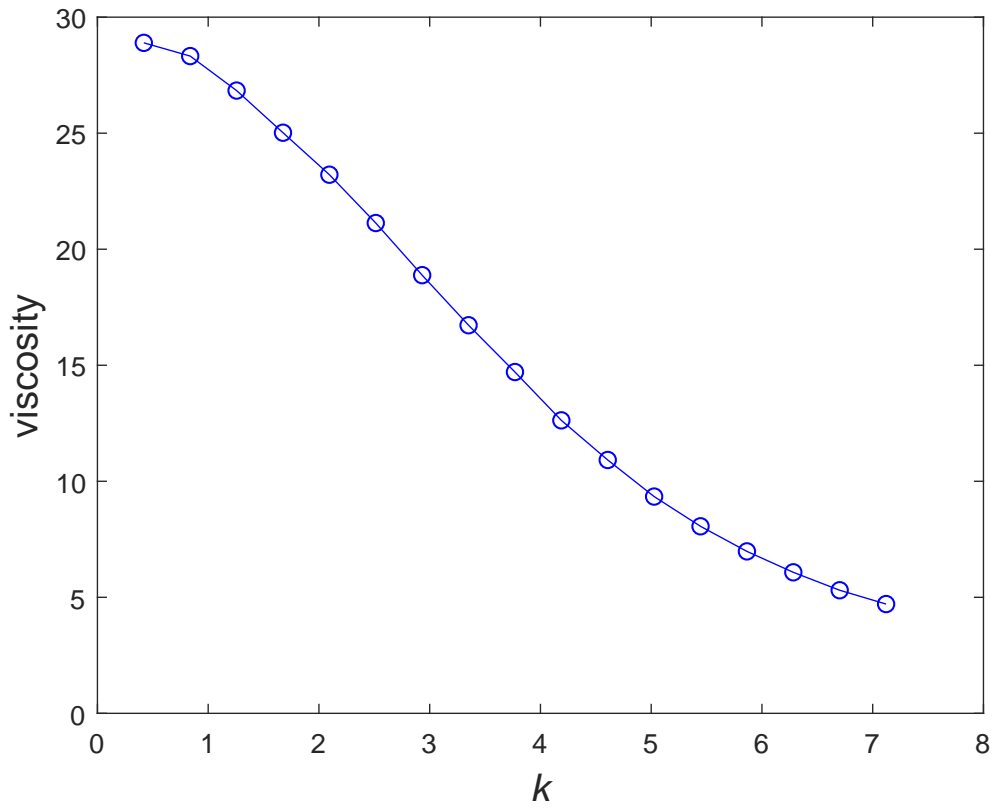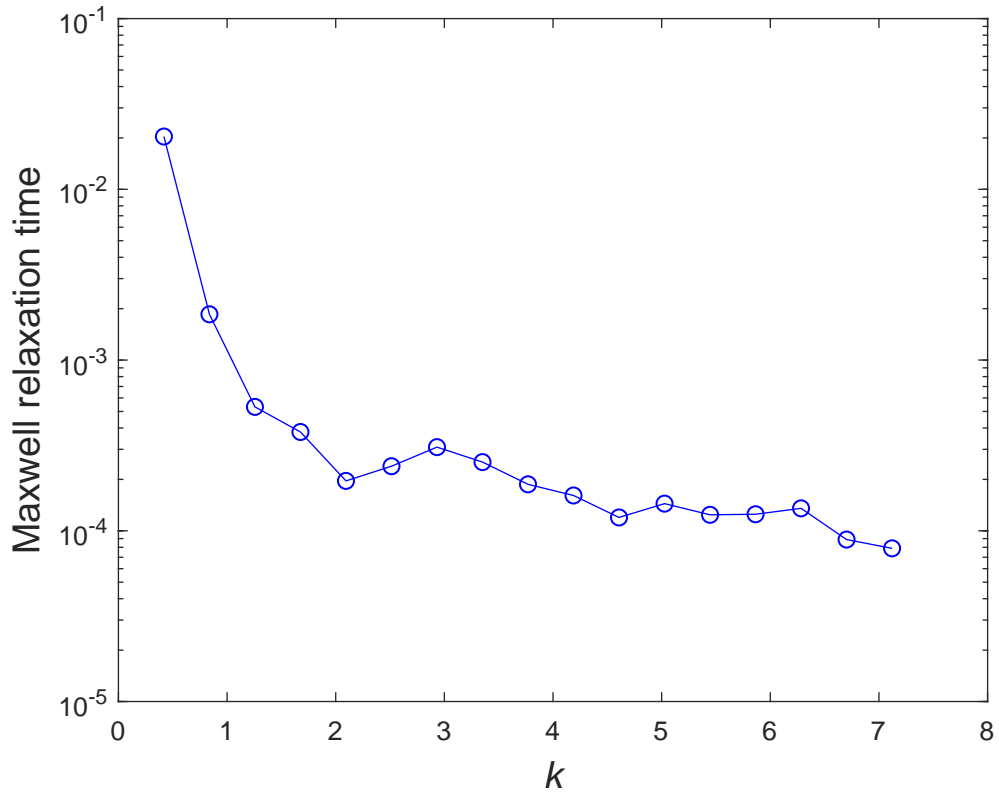
Figure 4: Viscoelastic fluids: The decay constant of the relaxation modulus and the viscosity as functions of the wave number. When k decreases, the decay constant has the tendency to increase quickly and is expected to reach its maximum in the hydrodynamic limit. For the shear viscosity η_k, the change is seen to be slow as $k \to 0$.
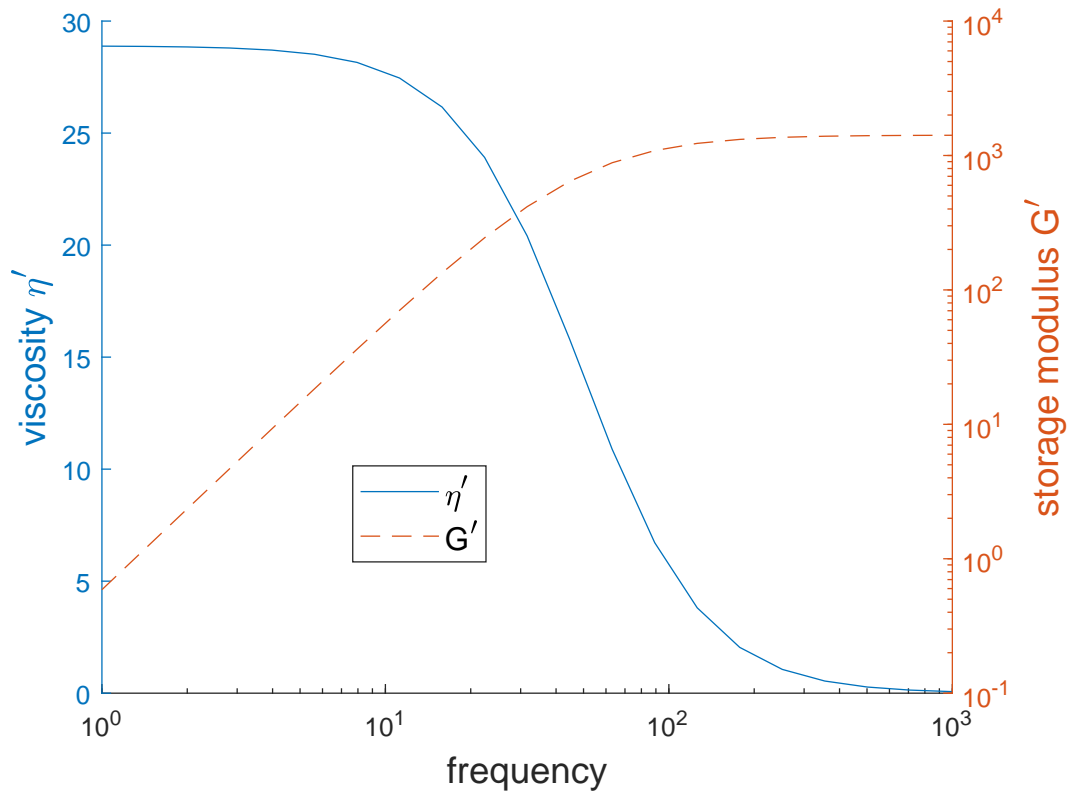
Figure 5: Viscoelastic fluids: Storage modulus and viscosity as functions of the frequency for the smallest wave number (i.e. $k = k_1 = 0.4189$). The system responses like a fluid at small values of the frequency (i.e. large observation time scale) and like a solid at large values of the frequency. The storage modulus provides a convenient means of quantifying the level of elasticity of the fluid.
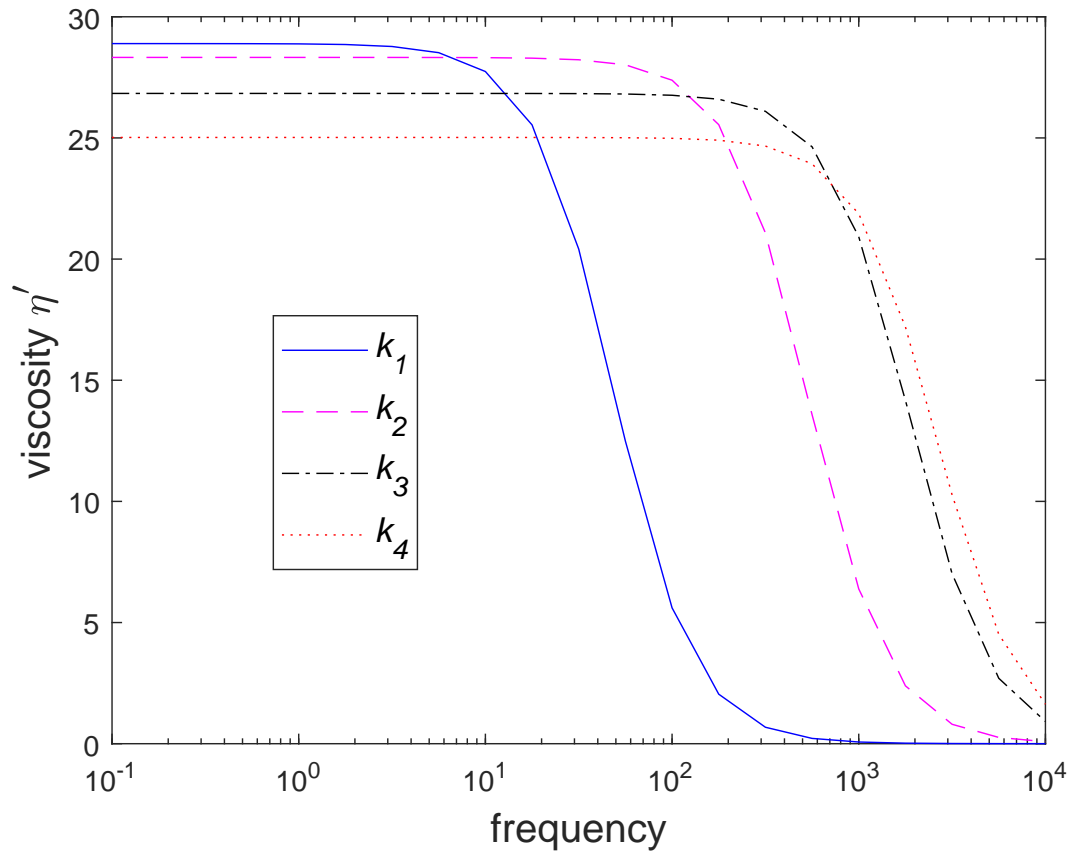
Figure 6: Viscoelastic fluids: Viscosity as a function of the frequency for the first four values of k (i.e. 0.4189, 0.8378, 1.2566 and 1.6755). It can be seen that $\eta' \to \eta_k$ (i.e. 28.8930, 28.3227, 26.8364, 25.0198) as $\omega \to 0$ and $\eta' \to 0$ as $\omega \to \infty$.
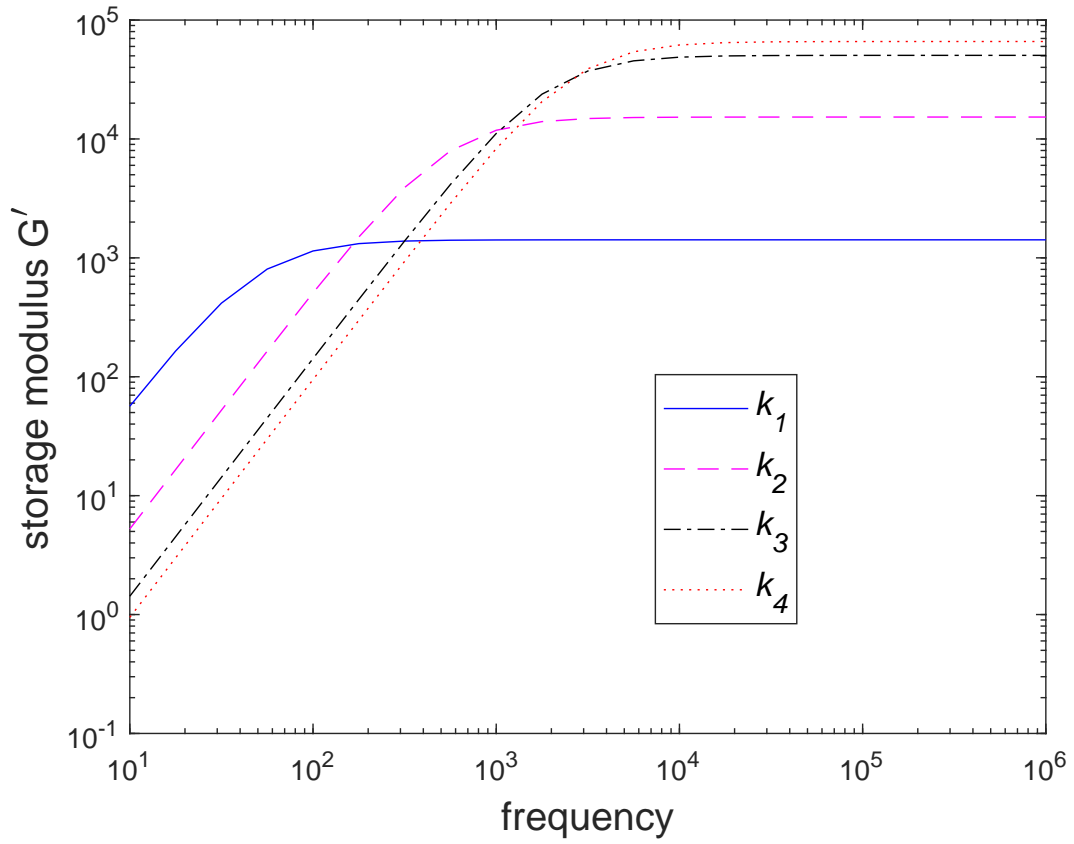
Figure 7: Viscoelastic fluids: Storage modulus as a function of the frequency for the first four values of k (i.e. 0.4189, 0.8378, 1.2566 and 1.6755). It can be seen that $G' \to 0$ as $\omega \to 0$ and $G' \to \eta_k/\tau_k$ (i.e. $1.4175 \times 10^3, 1.5283 \times 10^4, 5.0473 \times 10^4, 6.6011 \times 10^4$) as $\omega \to \infty$. In computing these limit values, the corresponding Maxwell relaxation times used are $\tau_k = (2.0383 \times 10^{-2}, 1.8532 \times 10^{-3}, 5.3170 \times 10^{-4}, 3.7902 \times 10^{-4})$.
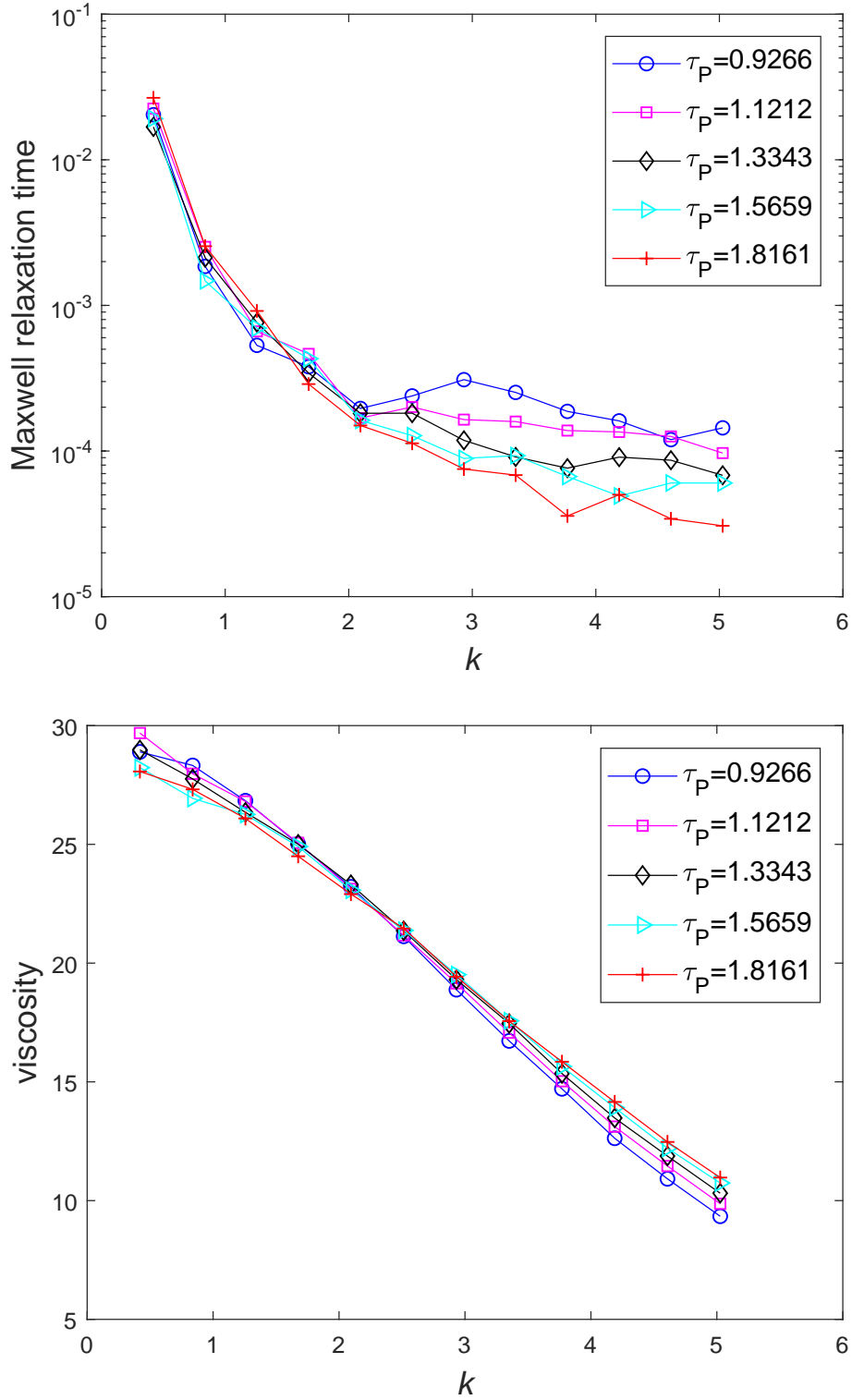
Figure 8: Viscoelastic fluids: As the wave number k is reduced, the relaxation times τ_k corresponding to different values of the particle diffusion time τ_P apparently converge. At finite k, the obtained results indicate that an increase in τ_P results in a decrease in τ_k. It can also be seen that a change in τ_P can affect the estimated viscosity at the hydrodynamic limit. All cases take $\rho = 4$, $S_c = 500$ and $\eta = 30$.
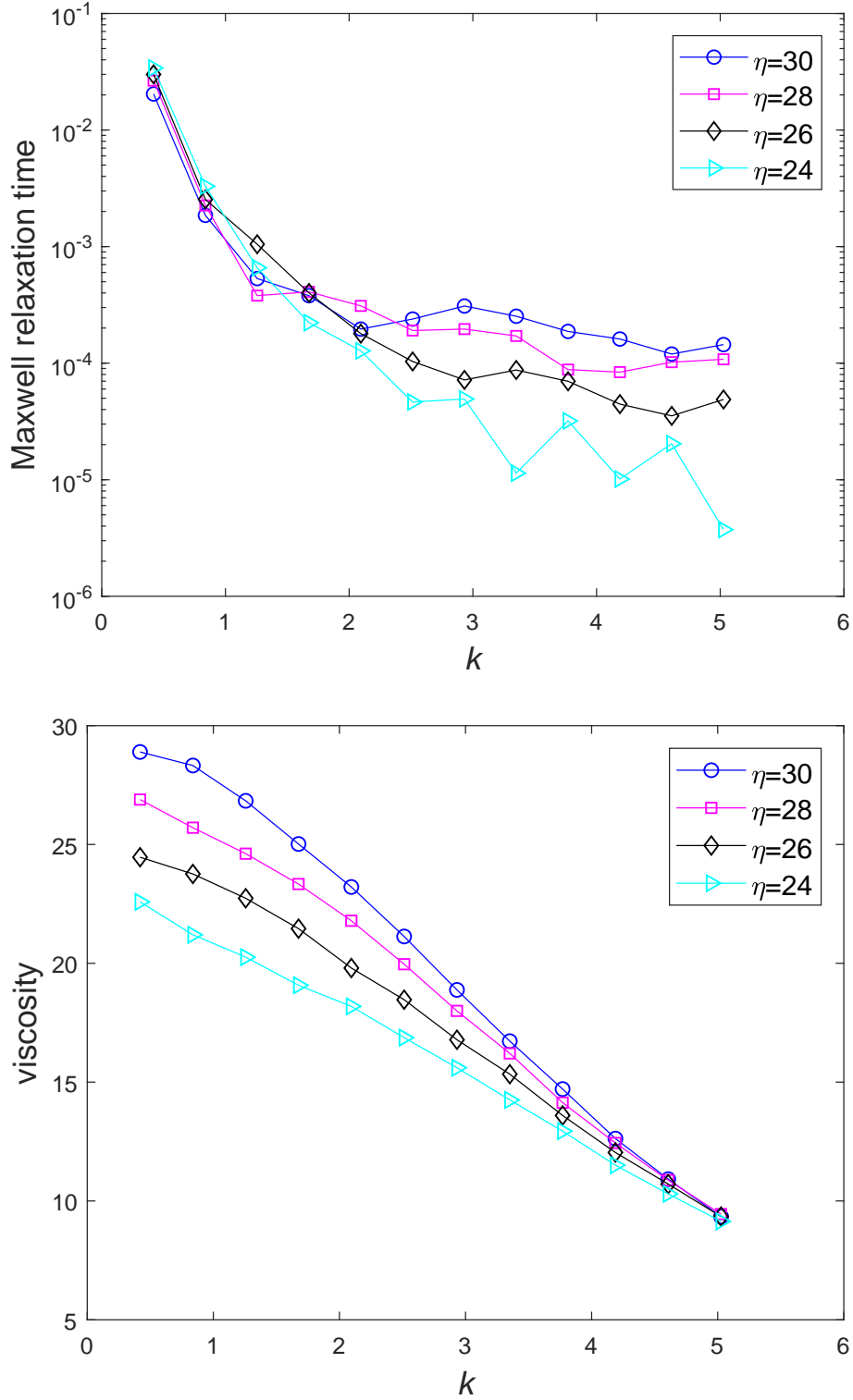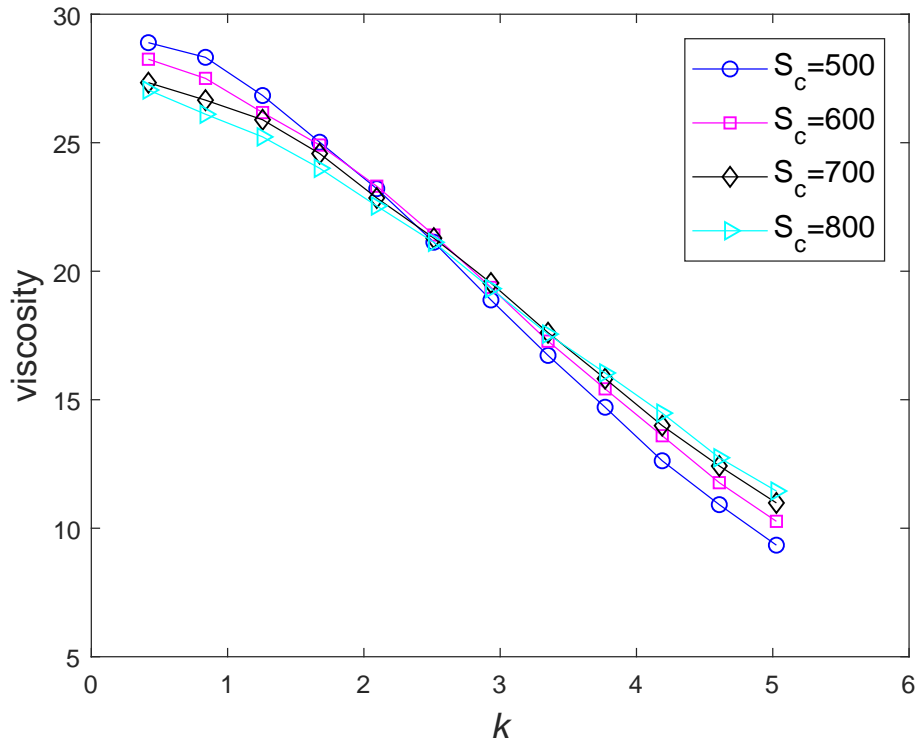
Figure 9: Viscoelastic fluids: As the wave number k is reduced, the relaxation times τ_k corresponding to different values of the imposed (limit) viscosity η apparently converge. At finite k, the obtained results indicate that a decrease in η results in a decrease in τ_k. All cases take $\rho = 4$, $S_c = 500$ and $k_B T = 1$.
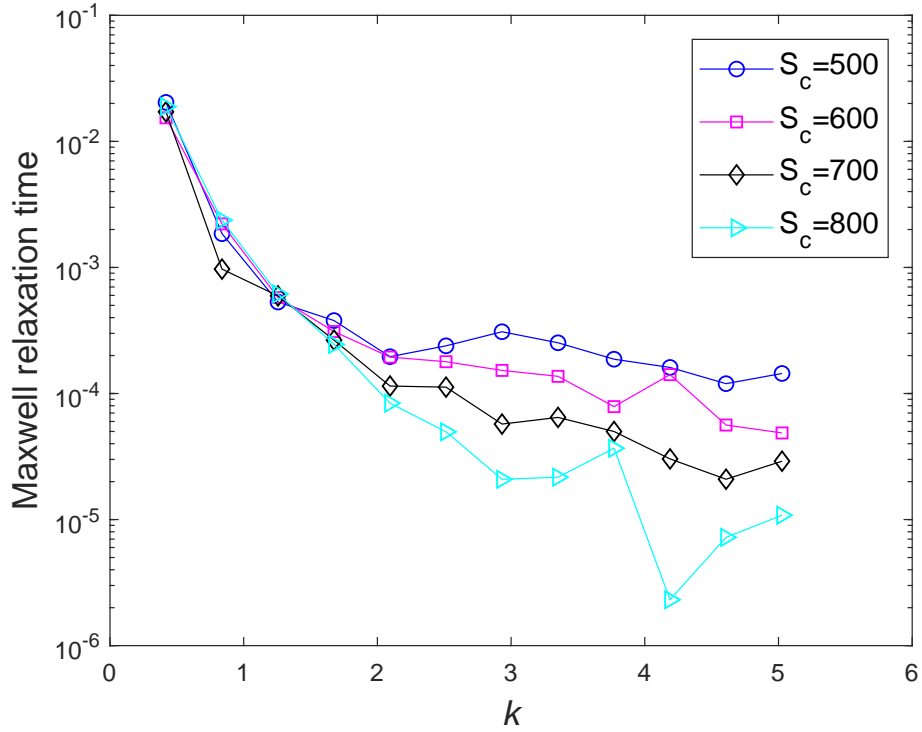
Figure 10: Viscoelastic fluids: As the wave number k is reduced, the relaxation times τ_k corresponding to different values of the imposed (limit) Schmidt number S_c apparently converge. At finite k, the obtained results indicate that an increase in S_c results in a decrease in τ_k. It can also be seen that a change in S_c can affect the estimated viscosity at the hydrodynamic limit. All cases take $\rho = 4$, $\eta = 30$ and $k_B T = 1$.